Automated measurement of permethylated serum N-glycans by MALDI–linear ion trap mass spectrometry

Maïlys Guillard [a], Jolein Gloerich [a,b], Hans J. C. T. Wessels [a,b], Eva Morava [c], Ron A. Wevers [a], Dirk J. Lefeber [a,*]

[a] Laboratory of Pediatrics and Neurology, Radboud University Nijmegen Medical Centre, PO Box 9101, 6500 HB, Nijmegen, The Netherlands
[b] Nijmegen Proteomics Facility, Radboud University Nijmegen Medical Centre, PO Box 9101, 6500 HB, Nijmegen, The Netherlands
[c] Department of Pediatrics, Radboud University Nijmegen Medical Centre, PO Box 9101, 6500 HB, Nijmegen, The Netherlands

ARTICLE INFO

ABSTRACT

The use of N-glycan mass spectrometry for clinical diagnostics requires the development of robust high-throughput profiling methods. Still, structural assignment of glycans requires additional information such as MS^2 fragmentation or exoglycosidase digestions. We present a setting which combines a MALDI ionization source with a linear ion trap analyzer. This instrumentation allows automated measurement of samples thanks to the crystal positioning system, combined with MS^n sequencing options. 2,5-Dihydroxybenzoic acid, commonly used for the analysis of glycans, failed to produce the required reproducibility due to its non-homogeneous crystallization properties. In contrast, α-cyano-4-hydroxycinnamic acid provided a homogeneous crystallization pattern and reproducibility of the measurements. Using serum N-glycans as a test sample, we focused on the automation of data collection by optimizing the instrument settings. Glycan structures were confirmed by MS^2 analysis. Although sample processing still needs optimization, this method provides a reproducible and high-throughput approach for measurement of N-glycans using a MALDI–linear ion trap instrument.

© 2009 Elsevier Ltd. All rights reserved.

1. Introduction

Protein glycosylation is one of the most common and complex post-translational modifications. Changes in the glycosylation pattern of specific or total serum proteins have proven to be useful as biomarkers for several diseases, including congenital disorders of glycosylation (CDG) and several forms of cancer.[1–4] For example, altered sialylation and fucosylation of N- and O-glycans, as determined by mass spectrometric profiling, have been related to the disease state.[4] Mass spectrometric analyses can either focus on global profiling of complex glycan mixtures or on structural determination of individual carbohydrates, including MS^n sequencing and linkage analysis.[5] For application of glycan profiling in a medical setting, reproducible, high-throughput methods are required to differentiate disease groups. Carbohydrate-deficient transferrin is used as biomarker for CDG.[6] Although isoelectric focusing of plasma transferrin is a convenient high-throughput method, the use of mass spectrometry of immunopurified transferrin provides increased sensitivity and additional structural information.[7–9] In a similar way, it can be expected that glycan profiling by mass spectrometry may prove helpful to determine the exact defect in CDGx patients.[8–11]

Mass spectrometry using MALDI has been applied successfully to glycan analysis because of its high sensitivity and the potential for high-throughput analysis.[12] It is less sensitive to residual contaminants such as salts compared to other ionization methods. Also, the ease of spectral interpretation facilitates unambiguous data analysis, as only singly charged ions are formed. Sialylated glycans have been analyzed in native form[13,14] after reductive amination[9,15,16] or after sialic acid methylesterification[11,17] or permethylation.[18–21] Permethylation of glycans, usually performed as described by Ciucanu and Kerek,[22] has several advantages, including increased stability of sialic acids, improved ionization efficiency, and ease of spectral interpretation since both acidic and neutral structures can be measured in the positive-ion mode.[12,21,23,24] A recent comparative study suggested that MALDI analysis of permethylated N-glycans and the analysis of reductively aminated glycans by HPLC can be correlated and are both reliable for the elucidation of glycan profiles.[23]

Most studies on N-glycan analysis by MALDI described the use of a MALDI ionization source with a time-of-flight analyzer, with the advantages of large mass range, high sensitivity, and high resolution. Structural assignment of glycans relies on MS^2 fragmentation options, as has been shown by the use of, for example, MALDI-TOF-TOF,[25,26] MALDI-QTOF for CDG-II patients,[9] MALDI-FTMS,[27–30]

* Corresponding author. Address: Laboratory of Pediatrics and Neurology, Institute for Genetic and Metabolic Disease, Radboud University Nijmegen Medical Centre, Geert Grooteplein 10, 6525 GA Nijmegen, The Netherlands. Tel.: +31 24 3614428; fax: +31 24 3618900.
E-mail address: D.Lefeber@cukz.umcn.nl (D.J. Lefeber).

and MALDI-ion trap.[31] The combination of soft ionization by MALDI with multistage MS is particularly well suited for the analysis of post-translationally modified peptides[32,33] and oligosaccharides.[2,31,34,35] Disassembly through a number of consecutive MS[n] stages allows structural distinction between ions with similar mass. For example, 13 methylated high-mannose isomers were distinguished from bovine ribonuclease B.[5] Fragmentation has also been used in order to gain insight in branching level, fucosylation site, and linkage of sialic acid.[25,26,35] MALDI analysis of carbohydrates has been extensively reviewed by Harvey.[4,36–38]

The matrix used for MALDI measurements is crucial for optimal signal-to-noise levels and the quality of data. 2,5-Dihydroxybenzoic acid (DHB) is most commonly used for measurement of permethylated glycans. It typically crystallizes as needle-shaped crystals along the border of the target spot. Luxembourg et al.[39] described that some crystals consist of matrix exclusively, while others contain mainly sodium and analyte or only sodium and little matrix. Different groups have tried to disrupt the large crystal formation by mixing DHB with other compounds such as aniline, *N,N*-dimethylaniline or glycerol,[40,41] or by recrystallization of the matrix using ice-cold ethanol.[42] α-Cyano-4-hydroxycinnamic acid (CHCA) is widely used as matrix for protein and peptide analyses, although Stephens et al.[43] described the use of CHCA to analyze fragmentation of native and permethylated oligosaccharides. Its crystallization pattern is much more homogeneous, which could be an advantage with respect to automated analysis. Various groups have analyzed the influence of matrix on glycan profile acquisition. Stephens et al.[43] showed that CHCA induces mainly fragmentation along the glycosidic bonds, whereas fragmentation using DHB as matrix causes a wide range of fragmentations. Creaser et al.[34] compared the efficiency of esculetin, CHCA, 2-(4′-hydroxyphenylazo)benzoic acid (HABA), DHB, and 2,4,6-trihydroxyacetophenone (THAP) in a quadrupole ion trap mass spectrometer. The use of HABA and esculetin provided increased sensitivity and a lesser degree of fragmentation compared to measurements using the other matrices.

In this study, we explored the potential of MALDI combined with a linear ion trap (LIT) (vMALDI-LTQ, Thermo Fisher Scientific) for the glycoprofiling of serum N-glycans with a focus on automated data acquisition. Apart from its advantage of possible MS[n] analysis, a number of unique features allows automated data collection of large numbers of samples, as required in a medical diagnostic setting. The crystal positioning system (CPS) automatically identifies matrix crystals on the target spot based on the image generated by a camera inside the MALDI source. It then generates an ideal path along the matrix crystals for the laser in order to collect sample data, avoiding places on the spot containing no crystals. This circumvents the need to manually scout the surface in order to hit the crystal-rich spots. In addition, the automatic gain control adjusts the number of laser shots needed to fill the ion trap.

Development of an efficient diagnostic workflow by means of mass spectrometry includes three steps: (i) optimization of sample processing prior to MS analysis, using very small amounts of biological material, (ii) accuracy, sensitivity, robustness, and high-throughput applicability of the measurement on the mass spectrometer, and (iii) automation of data processing. Here, we focused on the possibilities for automated data collection using a MALDI-LIT for measuring serum N-glycans.

2. Results and discussion

2.1. Choice of matrix for analysis of permethylated serum N-glycans

Permethylated N-glycans from total serum proteins were prepared as described in the experimental section. In initial experiments, DHB was used as matrix for measurement on the MALDI–LIT mass spectrometer. The detected glycan profile (Fig. 1a) showed the presence of major glycan ions at *m/z* 2432 and 2794, corresponding to mono- and disialylated biantennary N-glycans. Their fucosylated counterparts (*m/z* 2606 and 2968) were detected as well, along with a number of less abundant glycans. In addition, we observed an ion series with *m/z* values of 2739, 2494, 2132, 1914, and 1669 of unknown origin. The intensity of these ion peaks relative to each other remained fairly constant, while their collective appearance compared to the known glycans was highly variable within one spot. Optimization of instrument settings such as laser intensity did not result in elimination of these signals. The appearance of these unknown ions was unexpected since they were not detected when analyzing samples using DHB on a MALDI-TOF instrument operating in the reflectron mode (Fig. 1b), which suggests that they do not reflect sample or matrix contamination. The same peak series was detected for the commercial core fucosylated biantennary-disialylated A2F glycan (Fig. 1c).

A second observation with DHB was the irreproducibility of the signal intensity within one spot. Recording of 50 spectra within a single spot showed highly variable glycan ratios and a limited number of spectra with sufficient signal-to-noise ratios. Possibly, the needle-like crystallization pattern of DHB (Fig. 2) resulted in heterogeneous sample distribution along the spot, as has been described by Luxembourg et al.[39] Re-dissolving the crystallized matrix in ice-cold ethanol, followed by recrystallization or addition of glycerol to DHB as described by Soltwilsch et al.,[40] did not improve the homogeneity of the spot sufficiently.

In conclusion, automated data acquisition of permethylated serum N-glycans on the MALDI–LIT was not possible with DHB as the matrix. Therefore, other matrices were taken into consideration to obtain a homogeneous crystallization. Of these matrices, CHCA is commonly used for analysis of proteins and peptides and is known for its homogeneous analyte distribution.

Measurements of permethylated N-glycans using CHCA on a MALDI–LIT yielded spectra with specific glycan ion signals and high signal-to-noise ratio, whereas undesirable in- and post-source fragmentation ions were not observed. Of note, when using CHCA on a Bruker Biflex III MALDI-TOF instrument, no glycan signals could be observed using the same sample. To improve the homogeneity of the crystallization for use of the CPS, different spotting methods were studied. Premixing of dissolved analyte and CHCA matrix before spotting, mixing of the two solutions on the plate, or using the dried droplet method resulted in the formation of scattered crystal clusters. When the matrix was first spotted and allowed to dry before addition of the sample on top of it, a homogeneous crystal distribution was observed (Fig. 2), providing a larger surface area for measuring. The use of CPS still proved useful as empty spaces on the spot were not scanned by the laser, thereby avoiding the recording of spectra without a glycan signal. In this way, data could be automatically acquired.

2.2. Optimization of data collection on the MALDI–LIT instrument

To optimize the automated measurement of permethylated serum N-glycans, several instrumental parameters of the MALDI–LIT were adjusted. We investigated the path followed by the laser over the spot surface, the number of spectra recorded for each step, the number of sweep shots, and the use of automatic gain control. To assess the quality of a set of parameters, 50 spectra of one spot were recorded and screened manually. Settings were judged based on reproducibility of the spectra, signal-to-noise ratio, quality of the final averaged spectrum, and duration of analysis per spot. This led us to the following optimized measurement method. As the laser skims the surface of the spot, one spectrum was recorded
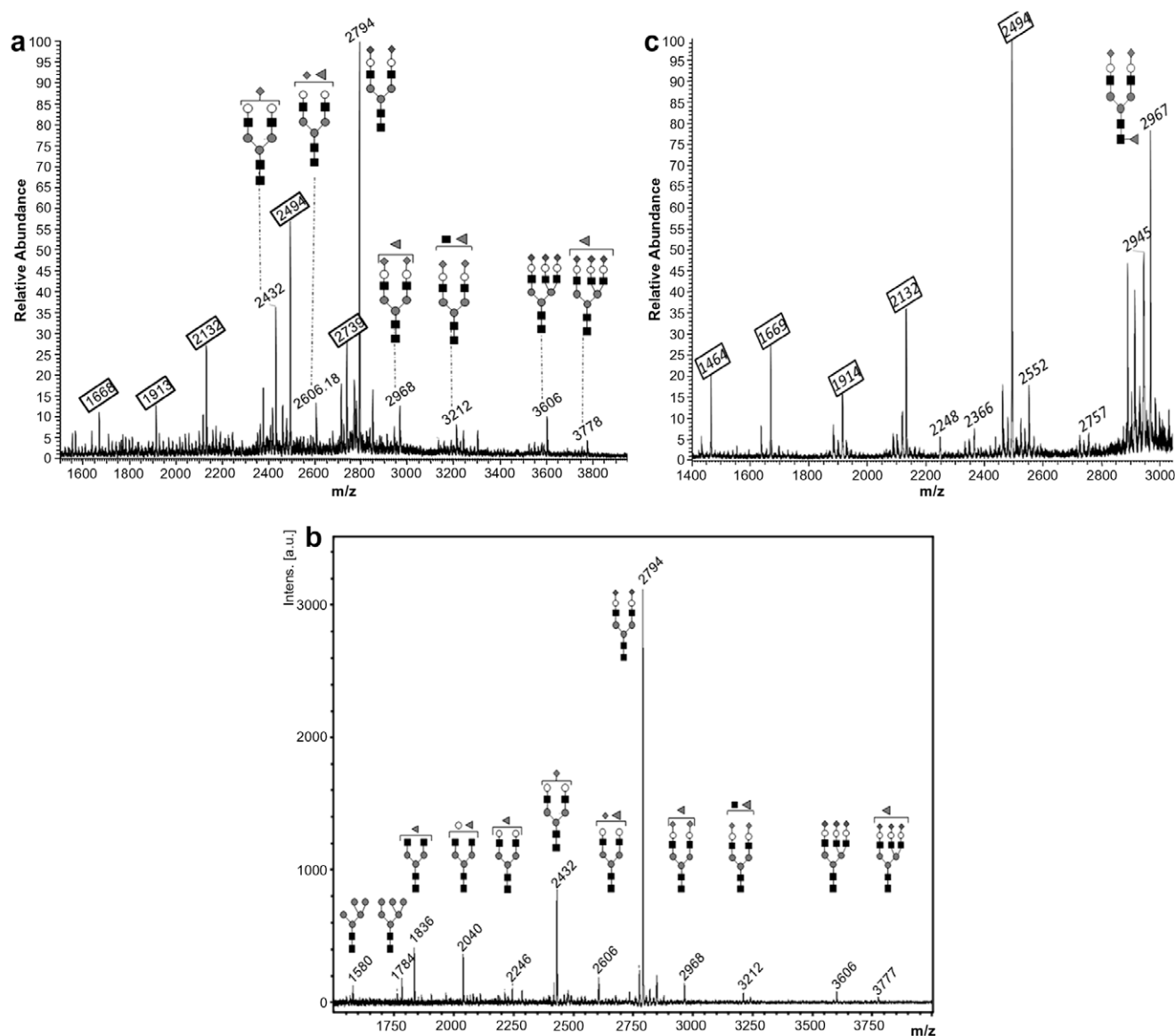
Figure 1. Analysis of permethylated N-glycans using DHB. A chosen set of glycan structures was assigned, fragment ion *m/z* values are boxed. (a) Serum N-glycans measured on MALDI–LIT, average of 100 spectra; (b) serum N-glycans measured by MALDI-TOF, fragment ions not detected; (c) MALDI–LIT spectrum of the A2F glycan standard showing fragment ions (■ = GlcNAc, ● = Man, ○ = Gal, ◆ = sialic acid, ▲ = Fuc).

for every step along the path as determined by the CPS. Each laser shot generating a spectrum is preceded by five unrecorded sweep shots in order to eliminate excess matrix. The spectra were recorded as survey scans in the high-mass mode (*m/z* 1500–4000) with two microscans and the automatic gain control enabled. An increased number of microscans or of recorded spectra for each step did not improve the reproducibility of the results, while it increased the overall measurement time. For each spot, 50 spectra were recorded and averaged. This improved the reliability of the averaged spectrum, as well as the signal-to-noise ratio. Using the optimized conditions (one spectrum per step, five sweep shots, and two microscans per spectrum for a total of 50 spectra), the analysis of one spot took 3–4 minutes.

2.3. The serum N-glycan profile

The final averaged spectrum reflects the general N-glycan profile of serum in line with previous publications[9,20,21,24] (Fig. 3). Gly-

can structures were confirmed on basis of MS[2] fragmentation patterns and common knowledge of the N-glycan biosynthetic pathway. The most abundant glycans included the disialylated-(*m/z* 2794) and monosialylated biantennary complex glycan (*m/z* 2432) and their fucosylated equivalents (*m/z* 2967 and 2606), as well as the trisialylated triantennary glycan (*m/z* 3606). Additional MS[2] fragmentation of minor signals revealed the presence of up to 40 additional glycan ions. The ratio of monosialo to disialo biantennary N-glycan (about 44%) and fucosylation levels were higher than those in published MALDI-TOF profiles of permethylated serum N-glycans.[20,21,24] Yet, the study of Ruhaak et al.[15] measuring 2-AA labeled glycans in the negative-ion mode also showed ratios of monosialo to disialo biantennary glycan higher than 40%. A comparative study on immunopurified transferrin[23] showed an estimated occurrence of roughly 10–45% monosialylated diantennary N-glycan compared to the total amount of disialylated diantennary N-glycan, as measured in seven different laboratories. The higher level of undersialylation in some laboratories was explained by a
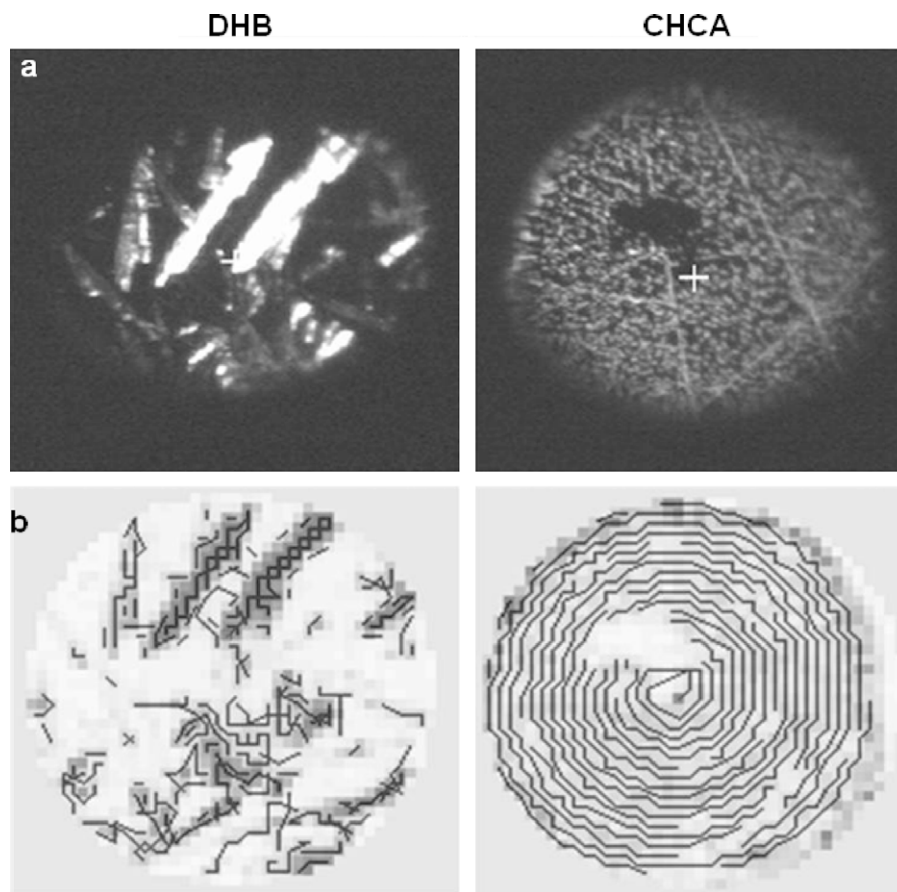
Figure 2. Crystallization pattern of different matrices. (a) Crystallization as detected by the charge-coupled camera of the MALDI and (b) signal of the crystal positioning system and generated path along the crystal surface.

probable sialic acid loss during sample preparation. Possibly, the use of different instrumentation results in slight variation of individual glycan ion intensities. Most previous studies were performed with time-of-flight analyzers, whereas we used a linear ion trap. Possibly, specific features of the ion trap may lead to differences in the data. In addition, although we found similar profiles for several control samples, variation in N-glycan composition between individuals could also partly explain the differences between studies. By HPLC, it has been shown that age, gender, and environmental determinants may affect the total serum N-glycan composition.[44] Glycan profiling of a larger number of individuals must be conducted to study the variability of glycans in healthy controls.

MS^2 spectra were generated by fragmenting selected precursor ions using collision-induced dissociation. This led to fragmentation of the glycan structures along the glycosidic bond, generating sodium-cationized B, C, Y, and Z ions (nomenclature according to Domon and Costello[45]). Analysis of the fragment ions confirmed the glycan nature of the precursor ions shown in Figure 3a. Fragmentation of the glycan ion with m/z 2968 (MS^2, Fig. 3b) generates essentially B and Y fragment ions. Also, $Y_{\alpha/\beta}$-ions, resulting from cleavage in both antennae, can be detected at, for example, m/z 1317.45 ($Y_{4\alpha/4\beta}$) and m/z 1592.45 ($Y_{4\alpha/6\beta}$). This MS^2 spectrum shows that fucosylation of the biantennary disialylated N-glycan occurs on both core and antenna N-acetylglucosamine (2-acetamido-2-deoxy-D-glucose) residues. The non-reducing end B-ions at m/z 1022.55 ($B_{4\alpha}$) and m/z 2690.09 (B_6) and the reducing end Y-ion at m/z 1968.82 ($Y_{4\alpha}$) are indicative of antenna fucosylation. In contrast, the $Y_{\alpha/\beta}$-ions at m/z 1113.36 ($Y_{3\alpha/4\beta}$) and m/z 1317.45

($Y_{4\alpha/4\beta}$), as well as the B-ion at m/z 2516.09 (B_6), indicate fucosylation of the chitobiose core. The MS^3 spectrum of m/z 1022 shows loss of sialic acid (m/z 646.18) and antenna fucose (m/z 815), thereby confirming the composition of this low-abundant MS^2 ion.

2.4. Reproducibility

To assess the reproducibility of our methods, we individually processed 10 aliquots of a control serum sample, as described in Section 3.4. These 10 aliquots were each spotted four times on the MALDI target plate. Data acquisition was performed by measuring each spot 50 times and averaging these spectra after outlier removal. A subset of 10 specific glycan ions (Table 1) was selected to assess reproducibility, in addition to the m/z 2794 ion used for normalization. The intensity of these glycan ions, relative to the m/z 2794 ion, was used for the calculation of the intra-spot variability, the inter-spot variability, and the inter-assay variability.

The intra-spot variability, or variability between measurements within one spot, was assessed by acquiring four data sets per spot on six spots of the same sample. For each spot, the relative intensities of the four acquisition sets were averaged, and the relative standard deviation (RSD) was calculated for our subset of glycan ions. The average RSD over the six spots was smaller than 10%, with slightly higher variability for small glycans (Table 1, column 4).

The inter-spot variability, or variability between data of four spots of the same aliquot measured on the same day, is represented in Figure 4. For each of the 10 glycan ions, the average intensity over the four spots was calculated with the RSD. In almost all cases, the inter-spot RSD was lower than 10%. Incidentally, mostly for low-
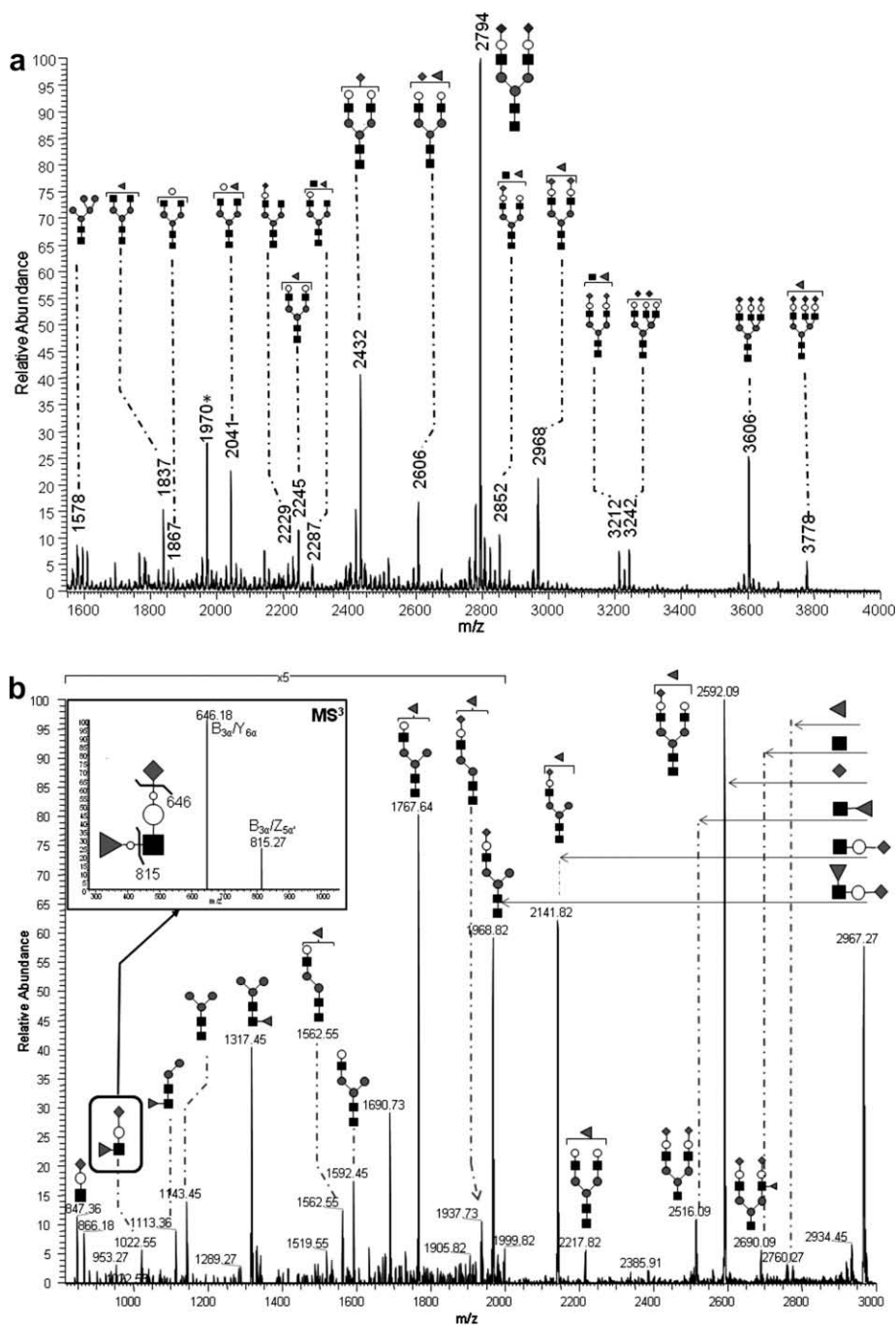
Figure 3. (a) Serum N-glycan as measured by MALDI–LIT using CHCA as matrix. Average of 50 spectra. Prominent glycans are assigned. (b) MS^2 CID spectrum of [M+Na]$^+$ precursor ion with m/z 2968. A number of potential fragment ions are labeled, loss of fragments from the precursor ion is indicated on the right side of the spectrum. Fragmen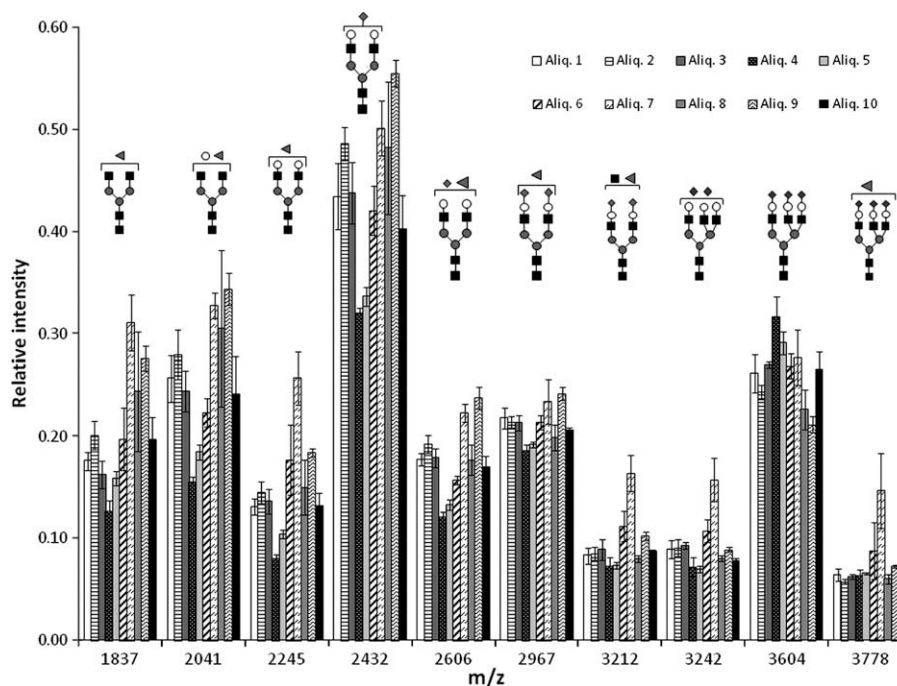ts with m/z 1022, 1143, and 2690 are indicative of antenna fucosylation, whereas fragments with m/z 1113, 1317, and 2516 implicate core fucosylation. MS^3 of the m/z 1022 ion confirms its proposed structure with terminal sialic acid and antenna fucosylation (■ = GlcNAc, ● = Man, ○ = Gal, ◆ = sialic acid, ▲ = Fuc).

abundant glycans, more variable intensities were found, with RSD ranging from 1.7% to 31%. This likely reflects the influence of higher background signals for these glycans. When averaged over the 10 aliquots, the RSD was lower than 10% for all glycan ions in our subset (Table 1 column 5). Comparable results have been reported in a study conducted by the HUPO Human Disease Glycomics/Proteome Initiative on transferrin and IgG N-glycans from human serum. Variability (n = 5) for analysis of permethylated N-glycans on these proteins using MALDI-TOF was less than 10% for major oligosaccharides and up to 34% for minor ones.[23]

Finally, the inter-assay variability, or variability between 10 aliquots processed from the same serum, was analyzed. For each aliquot, the ion intensities over the four spots were averaged. These intensities were then compared between the 10 aliquots, revealing inter-assay RSDs ranging from 8% to 36% (Table 1 column 6). Considering the high reproducibility of the MALDI measurement itself, this variability must be due to sample processing. Degradation and peeling reactions might be associated with high pH during the permethylation reaction of glycans,[18] while other steps in the purification of glycans may cause sialic acid loss or

Table 1
Relative glycan ion intensities (to *m/z* 2794) and RSD of serum N-glycans used for reproducibility assessment

Ion signal (*m/z*)	Glycan structure	Average relative ion signal	Average intra-spot RSD (*n* = 6) (%)	Average inter-spot RSD (*n* = 10) (%)	Inter-assay RSD (*n* = 10) (%)
1837		0.21	15	9.6	29
2041		0.26	15	8.8	23
2245		0.15	13	9.0	32
2432		0.44	8.5	5.7	17
2606		0.18	5.8	4.7	20
2968		0.21	4.7	3.8	8.2
3212		0.09	9.2	8.0	28
3242		0.09	7.8	7.4	27
3606		0.26	7.3	5.4	11
3778		0.07	7.8	9.8	36

Figure 4. Ten aliquots of one serum sample were processed independently, and each was measured on four spots. For a chosen subset of glycan ions, average relative intensities are presented with standard deviation (*n* = 4), in each one of these aliquots.

degradation of glycans. After independently processing serum N-glycans nine times, Kang et al. showed an average inter-assay RSD of 20% for the measurement of serum N-glycans,[24] ranging from 4.3% to 39%.

Overall, these results indicate that, while intra- and inter-spot variability are within acceptable range, sample processing still needs attention to further increase robustness and decrease inter-laboratory variability as required for a diagnostic test.

2.5. Conclusions

We have optimized a method for automatic data acquisition of serum N-glycans on a MALDI–LIT instrument. Homogeneous matrix crystallization has been proven essential for the reproducibility of the measurements. Although DHB is usually the matrix of choice for glycans, its needle-shaped crystal structure did not generate the desired level of reproducibility. However, by using CHCA, a highly reproducible measurement of serum N-glycans was set up. The crystal positioning system, along with other optimized instrument parameters, allowed the automation of data collection. Although the processing of glycans prior to measurement still needs optimization, this method provides a sensitive, robust, reproducible, and high-throughput method for analysis of N-glycans using a MALDI–LIT instrument.

3. Experimental

3.1. Materials

Serum was obtained from a healthy volunteer. HPLC-grade MeCN and MeOH were purchased from LabScan (Gliwice, Poland). NaOH pellets, CH₃I, and CHCl₃ were from Sigma–Aldrich Chemical Co. (Saint Louis, USA), anhyd DMSO was from Aldrich (Steinheim, Germany) and NaOAc·3H₂O was from E. Merck (Darmstadt, Germany). Trifluoroacetic acid (TFA) was from Riedel-deHaën (Saint-Louis, USA). Porous graphitized carbon SPE columns (3 mL, 250 mg) were purchased from Supelco (Steinheim, Germany), and the Sep-Pak C18 columns were from Waters (Milford, USA). Mass spectrometry grade 2,5-dihydroxybenzoic acid (DHB) and α-cyano-4-hydroxycinnamic acid (CHCA) were from Fluka (Steinheim, Germany). PNGase F kit was from New England Biolabs (Ipswich, USA). All water used was ultrapure.

3.2. Processing of glycans

N-glycans were released from serum glycoproteins using PNGase F mainly as described in the manufacturer's guide: a serum aliquot (10 μL) was diluted five times in saline, denaturing solution (11 μL) was added, and the sample was boiled (10 min). After addition of phosphate buffer (10×, 12 μL), NP40 (10×, 50 μL), and PNGase (5 μL), the mixture was incubated (37 °C, overnight). Released glycans were purified on porous graphitized carbon SPE columns as described.[46] The glycans were permethylated based on the method of Ciucanu and Kerek.[22] Ten NaOH pellets were crushed in DMSO (3 mL). To the dried glycans, 0.5 mL of the NaOH suspension and CH₃I (0.2 mL) were added. After incubation with shaking (10 min), the reaction was stopped by addition of water (1 mL). Water-soluble reagents were removed by liquid–liquid extraction with CHCl₃, and permethylated glycans were purified on a C18 Sep-Pak cartridge that was preconditioned sequentially using MeOH (5 mL), water (5 mL), MeCN (5 mL), and water (15 mL) prior to loading the sample. The sample was diluted in 50% aq MeOH and loaded onto the Sep-Pak column. After washing with water and 15% aq MeCN, the glycans were eluted using 75% aq MeCN and

dried. Spotting and measurement of each aliquot were performed immediately after processing.

3.3. Spotting

CHCA matrix was prepared by dissolving CHCA (5 mg/mL) in 1:1 (v/v) MeCN–20 mM aq NaOAc. DHB was dissolved (20 mg/mL) in 1:1 (v/v) MeOH–20 mM aq NaOAc. Fully processed permethylated glycans from 10 μL of serum were dissolved in 50 μL MeOH, then mixed 1:1 with 20 mM aq NaOAc. NaOAc was added to ensure generation of sodiated ions exclusively. First, matrix (0.5 μL) was spotted on one of the 384 sample wells of a stainless steel MALDI target plate. After crystallization, the sample (0.5 μL) was deposited on top of the matrix and allowed to dry at ambient temperature.

3.4. vMALDI-LTQ measurements, and data analysis

Glycan analyses were performed on a linear ion trap fitted with an intermediate pressure matrix-assisted laser-desorption ionization source (vMALDI LTQ, Thermo Fisher Scientific, San Jose, USA). The 337 nm N₂ laser (20 Hz, 250 μjoules per pulse) was located outside the instrument in a separate unit, and the laser beam was directed to the vMALDI source through a fiberoptic cable. Its power could be adjusted through an iris attenuator. As transmission may degrade over time due to buildup of material in the fiberoptic cable, the laser power was optimized before each set of measurements. The mass analyzer was a standard LTQ with vMALDI source modifications that included a camera, *x,y*-table, sample plate, quadrupole q00 with auxiliary rods, and skimmer. Ions generated by the MALDI process are guided to the linear ion trap via a differentially pumped multipole assembly. It is important to note that the intermediate pressure of the vMALDI source is several orders of magnitude higher compared to traditional vacuum MALDI.[47] Ions generated by traditional vacuum MALDI have high internal energies that may lead to in- or post-source decay (ISD/PSD) of excited ions. Although both ISD and PSD are useful techniques to characterize ions, unwanted fragmentation of analyte ions makes the analyses of labile molecules (i.e., phosphopeptides) rather ambiguous. It has been shown previously that elevated pressures reduce source fragmentation of analyte ions by a process called collisional cooling: ions generated by MALDI have relatively high internal energies (influenced by the matrix type) but are cooled down by gas-phase collisions that lower the internal energy of the analyte ion and return its internal energy level back to the ground state.[47,48]

In the optimized setting, CPS and AGC were enabled. One spectrum was recorded for each step along the CPS-pathway. To improve the signal-to-noise ratio and the reliability of this spectrum, two measurements, or so-called microscans, were averaged each time. Only ions with *m/z* between 1500 and 4000 were measured, smaller ions were removed by the q00 octopole before reaching the ion trap. Mass spectra were acquired automatically, based on a sequence of spots programmed into the control software Xcalibur 2.0 SR2 (Thermo Fisher Scientific, 1998–2006). MS² data were generated for selected precursor ions using collision-induced dissociation at 35% laser power. Assignment of the fragment structures was calculated based on differences of molecular weight between ions. GlycoWorkBench[49] was used for support in the annotation of fragments, and fragments were assigned using the nomenclature by Domon and Costello.[45] MALDI-TOF measurements were performed on a Bruker III mass spectrometer set to the reflectron mode. A malto-oligosaccharide mixture was used for calibration. The number of spectra summed depended on signal intensity.

Spectral data were parsed from raw data files as comma separated CSV files using the MASIC software tool developed by Monroe et al.[50] The masic software (version 2.5.3050.16636, Richland, USA) was used as the parser, since this publicly available software tool is capable of handling data formats from mass spectrometers developed by different manufacturers. An in-house developed Perl script was used to process the exported data for further analysis. This script imports all raw spectral points and (i) extracts intensities for peaks of interest, (ii) normalizes the intensity of each *m/z* value of interest to a preselected *m/z* value within each spectrum, (iii) iteratively performs a Grubbs' test for selected *m/z* values to remove outliers at a 95% confidence level, and (iv) reports the average intensities and standard deviations for selected *m/z* values (before and after outlier removal) as well as average signal-to-noise ratios after outlier removal. On average, 5–10% of the spectra were removed by the outlier removal tool, improving the reliability of the remaining spectra. These spectra usually showed very low signal-to-noise ratios, due to lack of analyte, excess of matrix, or bad crystallization at a certain place on the spot.

Acknowledgments

References

1. Kam, R. K.; Poon, T. C.; Chan, H. L.; Wong, N.; Hui, A. Y.; Sung, J. J. *Clin. Chem.* **2007**, *53*, 1254–1263.
2. Zhao, J.; Simeone, D. M.; Heidt, D.; Anderson, M. A.; Lubman, D. M. *J. Proteome Res.* **2006**, *5*, 1792–1802.
3. Alavi, A.; Axford, J. S. *Dis. Markers* **2008**, *25*, 193–205.
4. Harvey, D. J. *Mass Spectrom. Rev.* **2009**, *28*, 273–361.
5. Prien, J. M.; Ashline, D. J.; Lapadula, A. J.; Zhang, H.; Reinhold, V. N. *J. Am. Soc. Mass Spectrom.* **2009**, *20*, 539–556.
6. Marklova, E.; Albahri, Z. *Clin. Chim. Acta* **2007**, *385*, 6–20.
7. Wada, Y.; Nishikawa, A.; Okamoto, N.; Inui, K.; Tsukamoto, H.; Okada, S.; Taniguchi, N. *Biochem. Biophys. Res. Commun.* **1992**, *189*, 832–836.
8. Wada, Y. *J. Chromatogr., B Anal. Technol. Biomed. Life Sci.* **2006**, *838*, 3–8.
9. Butler, M.; Quelhas, D.; Critchley, A. J.; Carchon, H.; Hebestreit, H. F.; Hibbert, R. G.; Vilarinho, L.; Teles, E.; Matthijs, G.; Schollen, E.; Argibay, P.; Harvey, D. J.; Dwek, R. A.; Jaeken, J.; Rudd, P. M. *Glycobiology* **2003**, *13*, 601–622.
10. Barone, R.; Sturiale, L.; Garozzo, D. *Mass Spectrom. Rev.* **2008**, *28*, 517–542.
11. Sagi, D.; Kienz, P.; Denecke, J.; Marquardt, T.; Peter-Katalinic, J. *Proteomics* **2005**, *5*, 2689–2701.
12. Haslam, S. M.; North, S. J.; Dell, A. *Curr. Opin. Struct. Biol.* **2006**, *16*, 584–591.
13. Mills, P.; Mills, K.; Clayton, P.; Johnson, A.; Whitehouse, D.; Winchester, B. *Biochem. J.* **2001**, *359*, 249–254.
14. Mills, P. B.; Mills, K.; Johnson, A. W.; Clayton, P. T.; Winchester, B. G. *Proteomics* **2001**, *1*, 778–786.
15. Ruhaak, L. R.; Huhn, C.; Waterreus, W. J.; de Boer, A. R.; Neususs, C.; Hokke, C. H.; Deelder, A. M.; Wuhrer, M. *Anal. Chem.* **2008**, *80*, 6119–6126.
16. Thaysen-Andersen, M.; Mysling, S.; Hojrup, P. *Anal. Chem.* **2009**, *81*, 3933–3943.
17. Kranz, C.; Denecke, J.; Lehrman, M. A.; Ray, S.; Kienz, P.; Kreissel, G.; Sagi, D.; Peter-Katalinic, J.; Freeze, H. H.; Schmid, T.; Jackowski-Dohrmann, S.; Harms, E.; Marquardt, T. *J. Clin. Invest.* **2001**, *108*, 1613–1619.
18. Kang, P.; Mechref, Y.; Kyselova, Z.; Goetz, J. A.; Novotny, M. V. *Anal. Chem.* **2007**, *79*, 6064–6073.
19. Kang, P.; Mechref, Y.; Klouckova, I.; Novotny, M. V. *Rapid Commun. Mass Spectrom.* **2005**, *19*, 3421–3428.
20. Faid, V.; Chirat, F.; Seta, N.; Foulquier, F.; Morelle, W. *Proteomics* **2007**, *7*, 1800–1813.
21. Morelle, W.; Michalski, J. C. *Nat. Protocols* **2007**, *2*, 1585–1602.
22. Ciucanu, I.; Kerek, F. *Carbohydr. Res.* **1984**, *131*, 209–217.
23. Wada, Y.; Azadi, P.; Costello, C. E.; Dell, A.; Dwek, R. A.; Geyer, H.; Geyer, R.; Kakehi, K.; Karlsson, N. G.; Kato, K.; Kawasaki, N.; Khoo, K. H.; Kim, S.; Kondo, A.; Lattova, E.; Mechref, Y.; Miyoshi, E.; Nakamura, K.; Narimatsu, H.; Novotny, M. V.; Packer, N. H.; Perreault, H.; Peter-Katalinic, J.; Pohlentz, G.; Reinhold, V. N.; Rudd, P. M.; Suzuki, A.; Taniguchi, N. *Glycobiology* **2007**, *17*, 411–422.
24. Kang, P.; Mechref, Y.; Novotny, M. V. *Rapid Commun. Mass Spectrom.* **2008**, *22*, 721–734.
25. Babu, P.; North, S. J.; Jang-Lee, J.; Chalabi, S.; Mackerness, K.; Stowell, S. R.; Cummings, R. D.; Rankin, S.; Dell, A.; Haslam, S. M. *Glycoconjugate J.* **2008**, Epub ahead of print.
26. Mechref, Y.; Kang, P.; Novotny, M. V. *Rapid Commun. Mass Spectrom.* **2006**, *20*, 1381–1389.
27. Solouki, T.; Reinhold, B. B.; Costello, C. E.; O'Malley, M.; Guan, S.; Marshall, A. G. *Anal. Chem.* **1998**, *70*, 857–864.
28. An, H. J.; Miyamoto, S.; Lancaster, K. S.; Kirmiz, C.; Li, B.; Lam, K. S.; Leiserowitz, G. S.; Lebrilla, C. B. *J. Proteome Res.* **2006**, *5*, 1626–1635.
29. Lancaster, K. S.; An, H. J.; Li, B.; Lebrilla, C. B. *Anal. Chem.* **2006**, *78*, 4990–4997.
30. Kirmiz, C.; Li, B.; An, H. J.; Clowers, B. H.; Chew, H. K.; Lam, K. S.; Ferrige, A.; Alecio, R.; Borowsky, A. D.; Sulaimon, S.; Lebrilla, C. B.; Miyamoto, S. *Mol. Cell Proteomics* **2007**, *6*, 43–55.
31. Haebel, S.; Bahrke, S.; Peter, M. G. *Anal. Chem.* **2007**, *79*, 5557–5566.
32. Britton, D. J.; Scott, G. K.; Schilling, B.; Atsriku, C.; Held, J. M.; Gibson, B. W.; Benz, C. C.; Baldwin, M. A. *J. Am. Soc. Mass Spectrom.* **2008**, *19*, 729–740.
33. Atsriku, C.; Benz, C. C.; Scott, G. K.; Gibson, B. W.; Baldwin, M. A. *Anal. Chem.* **2007**, *79*, 3083–3090.
34. Creaser, C. S.; Reynolds, J. C.; Harvey, D. J. *Rapid Commun. Mass Spectrom.* **2002**, *16*, 176–184.
35. Devakumar, A.; Mechref, Y.; Kang, P.; Novotny, M. V.; Reilly, J. P. *Rapid Commun. Mass Spectrom.* **2007**, *21*, 1452–1460.
36. Harvey, D. J. *Mass Spectrom. Rev.* **2008**, *27*, 125–201.
37. Harvey, D. J. *Mass Spectrom. Rev.* **2006**, *25*, 595–662.
38. Harvey, D. J. *Mass Spectrom. Rev.* **1999**, *18*, 349–450.
39. Luxembourg, S. L.; McDonnell, L. A.; Duursma, M. C.; Guo, X.; Heeren, R. M. *Anal. Chem.* **2003**, *75*, 2333–2341.
40. Soltwisch, J.; Berkenkamp, S.; Dreisewerd, K. *Rapid Commun. Mass Spectrom.* **2008**, *22*, 59–66.
41. Snovida, S. I.; Perreault, H. *Rapid Commun. Mass Spectrom.* **2007**, *21*, 3711–3715.
42. Harvey, D. J. *Rapid Commun. Mass Spectrom.* **1993**, *7*, 614–619.
43. Stephens, E.; Maslen, S. L.; Green, L. G.; Williams, D. H. *Anal. Chem.* **2004**, *76*, 2343–2354.
44. Knezevic, A.; Polasek, O.; Gornik, O.; Rudan, I.; Campbell, H.; Hayward, C.; Wright, A.; Kolcic, I.; O'Donoghue, N.; Bones, J.; Rudd, P. M.; Lauc, G. *J. Proteome Res.* **2009**, *8*, 694–701.
45. Domon, B.; Costello, C. E. *Glycoconjugate J.* **1988**, *5*, 397–409.
46. Packer, N. H.; Lawson, M. A.; Jardine, D. R.; Redmond, J. W. *Glycoconjugate J.* **1998**, *15*, 737–747.
47. Garrett, T. J.; Yost, R. A. *Anal. Chem.* **2006**, *78*, 2465–2469.
48. Gil, G. C.; Kim, Y. G.; Kim, B. G. *Anal. Biochem.* **2008**, *379*, 45–59.
49. Ceroni, A.; Maass, K.; Geyer, H.; Geyer, R.; Dell, A.; Haslam, S. M. *J. Proteome Res.* **2008**, *7*, 1650–1659.
50. Monroe, M. E.; Shaw, J. L.; Daly, D. S.; Adkins, J. N.; Smith, R. D. *Comput. Biol. Chem.* **2008**, *32*, 215–217.